Journal of Crystal Growth 414 (2015) 119–122

Contents lists available at ScienceDirect

Journal of Crystal Growth

journal homepage: www.elsevier.com/locate/jcrysgro

MOVPE grown periodic AlN/BAlN heterostructure with high boron content

X. Li [a,b], S. Sundaram [b], Y. El Gmili [b], F. Genty [c], S. Bouchoule [d], G. Patriache [d], P. Disseix [e], F. Réveret [e], J. Leymarie [e], J.-P. Salvestrini [b,f], R.D. Dupuis [g], P.L. Voss [a,b], A. Ougazzaden [a,b,*]

[a] School of Electrical and Computer Engineering, Georgia Institute of Technology, GT-Lorraine, 57070 Metz, France
[b] UMI 2958, Georgia Tech - CNRS, 57070 Metz, France
[c] Supelec, LMOPS, EA 4423, 57070 Metz, France
[d] LPN CNRS, UPR20, 91460 Marcoussis, France
[e] Institut Pascal UMR 6602 CNRS, Université Blaise Pascal, 63171 Aubière, France
[f] Université de Lorraine, LMOPS, EA 4423, 57070 Metz, France
[g] Center for Compound Semiconductors and School of Electrical and Computer Engineering, Georgia Institute of Technology, Atlanta, GA 30332, USA

ARTICLE INFO

Available online 28 September 2014

Keywords:
A3. MOVPE
B1. III-nitrides
B1. Boron
B1. BAlN

ABSTRACT

Five-period AlN/BAlN heterostructure containing boron as high as 11% has been successfully grown by MOVPE. Good periodicity of two alternative layers has been observed by both SIMS profile and *Z*-contrast HAADF-STEM images. The BAlN layers demonstrate columnar polycrystalline feature. The BAlN layers exhibit an emission peak by CL and absorption edge in transmission spectra at around 260 nm. The results enable the development of BAlGaN based multi-layered heterostructure for UV and deep UV applications.

1. Introduction

III-nitrides are excellent wide bandgap semiconductors which exhibit thermal stability, high thermal conductivity, mechanical strength and chemical stability. These interesting properties promote their applications for optoelectronic devices in deep UV region and also high power high frequency electronics. Besides the conventional AlGaInN system, the BAlGaN system can offer large versatility for bandgap, lattice and refractive index engineering. For instance, it is possible to decrease or eliminate lattice mismatch on SiC and AlN substrates by introducing boron [1–3]. Especially, it has been experimentally proved that a small amount of boron incorporation in AlN can introduce a strong refractive index contrast [4]. Hence the BAlGaN system has been recently proposed as a promising candidate for Distributive Bragg Reflector (DBR) applied in deep UV vertical cavity surface emitting lasers (VCSELs) [5,6]. However, challenges lie in the growth of this material. Phase separation would happen due to large bond mismatch of BN and other nitrides, and crystallinity was limited because of short diffusion length of boron and strong parasitic reaction in the gas phase [7–9].

Most of the studies concentrate on BAlN single layers with only 1–2% boron. High boron containing layers growth by MOVPE has not been progressed a lot, which might be because the growth is normally performed at 1000 °C or above [2,4,10,11] in order to enhance B atoms diffusion, but at this high temperature the B-rich phase would poison the growth under high TEB/III ratio [12,13]. Low growth temperature can alleviate this problem and high boron incorporation can be achieved [13], but it does not facilitate growth of AlN for heterostructures or AlGaN MQWs. The fabrication of heterostructure is an important issue which needs to be further developed no matter for BAlGaN based MQWs or for DBRs.

This work reports on the growth and characterizations of 5-period AlN/BAlN heterostructure grown by metal–organic vapor phase epitaxy (MOVPE). The BAlN layers contain high boron content of 11%. Crystalline features and the optical properties of this heterostructure have been studied.

2. Experiments

5-period AlN/BAlN layers (25 nm / 32 nm) were grown in a MOVPE T-shape reactor [14] at 100 Torr by using hydrogen as carrier gas. The growth was performed on two types of substrates: 1 μm AlN templates on sapphire and 3 μm GaN templates on sapphire. The AlN templates are appropriate substrates for deep UV applications while GaN templates are used as reference. The temperature was maintained at 1000 °C during the growth and TEB/III molar ratio in the vapor phase was 40% in order to have high boron incorporation. Flow-

* Corresponding author. Tel.: + 33 3 87 20 39 23; fax: + 33 3 87 20 39 40.
E-mail address: aougazza@georgiatech-metz.fr (A. Ougazzaden).

http://dx.doi.org/10.1016/j.jcrysgro.2014.09.030
0022-0248/

modulate epitaxy (FME) was applied during the growth of BAlN layers in order to enhance the migration of B and Al atoms, and also suppress parasitic reactions [9–11]. 2 s supply of metal–organics and 1 s supply of NH_3 were alternatively run into the reactor without interruption [9,10]. The AlN layers were grown in a continuous way. A schematic of precursors feeding sequence for BAlN and AlN is presented in Fig. 1

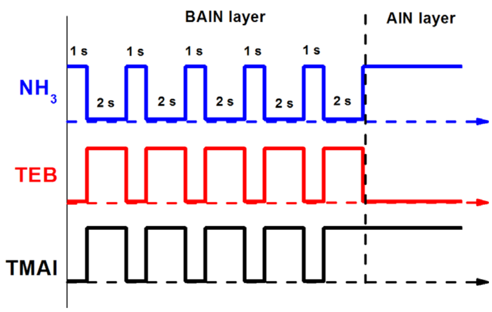

Fig. 1. Schematic of precursors feeding sequence for BAlN and AlN.

The depth concentration profiles for Al, B, N were performed by secondary ion mass spectroscopy (SIMS). The boron content in BAlN solid layer was estimated by using a B implanted AlN reference sample as quantitative calibration. The cross-section and interfaces of heterostructure were examined by High-angle Annular Dark Field Scanning Transmission Microscopy (HAADF-STEM) performed on an aberration-corrected JEOL 2200FS electron transmission microscopy. High resolution X-ray diffraction (XRD) measurements were performed in a Panalytical X'pert Pro MRD system with Cu QUOTE radiation. Surface morphology was characterized by atomic force microscope (AFM). Optical properties were investigated by cathodoluminescence and transmission spectra.

3. Results and discussion

3.1. Boron concentration analysis

The boron concentration in the BAlN layers along growth direction was evaluated by SIMS profiles, as shown in Fig. 2(a). It is clear that B profile varies anti-phase with Al. The Al signal

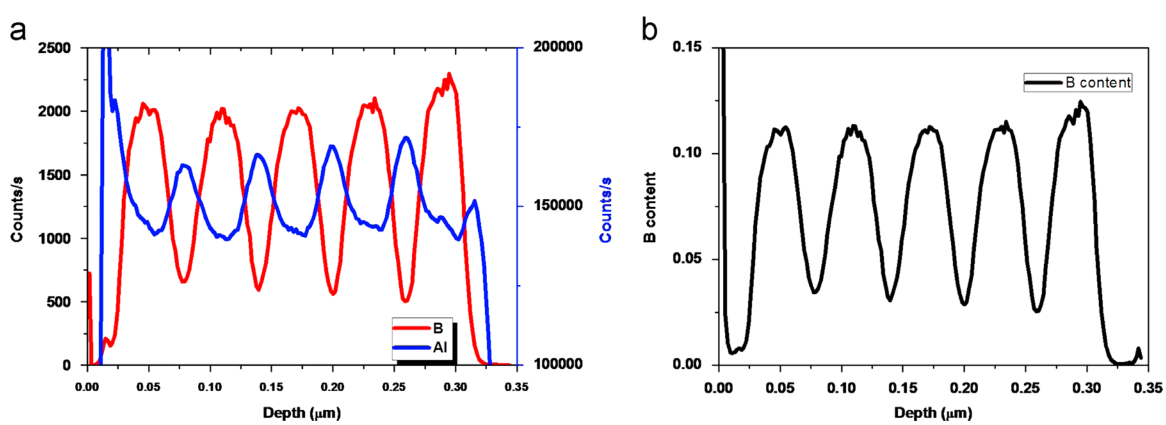

Fig. 2. (a) SIMS elemental concentration depth profiles of B and Al for the sample grown on GaN template, (b) Boron content in solid layers calculated from SIMS by using boron implanted AlN sample as reference.

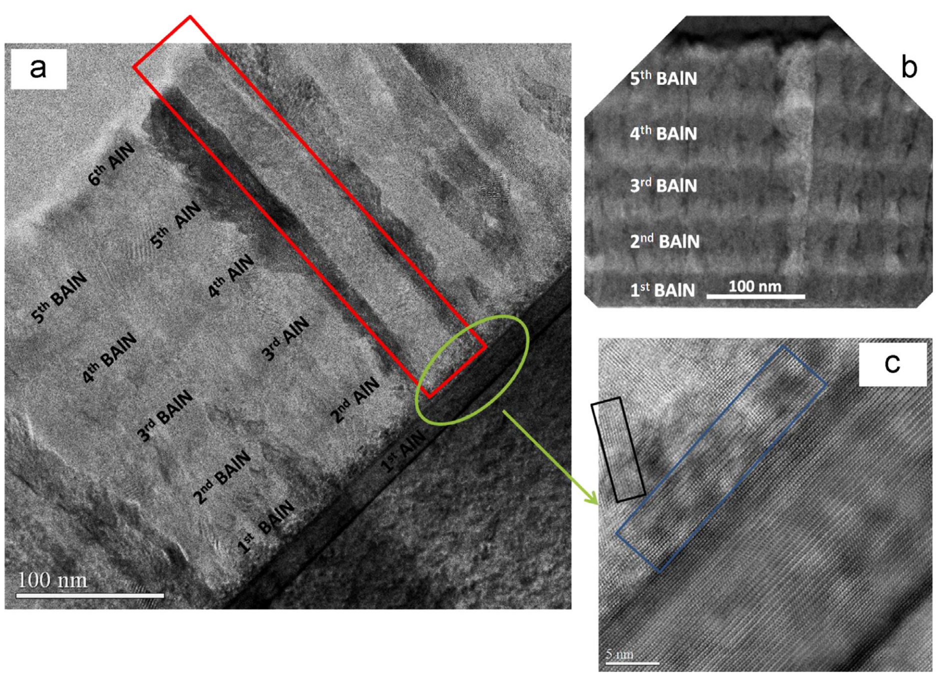

Fig. 3. (a) STEM images (bright-field) of 5-period AlN/BAlN heterostructure grown on AlN template and columns are clearly observed in the structure; (b) HAADF–STEM image to show better contrast of BAlN and AlN layers; and (c) high magnification of the zone where the 1st BAlN layer starts to grow.

intensity decreases when boron signal intensity increases during BAlN growth, which indicates that boron atoms substitute Al atoms on the III sites of lattice to form BAlN alloy. 5-period AlN/BAlN layers exhibit good uniformity except that the first AlN layer has lower AlN intensity which is due to some Ga contamination from the sample holder and reactor [15]. It should be pointed out that the boron signal cannot be zero when it is sputtered into AlN layer considering the SIMS detection limit when thin layers are analyzed. In order to calibrate SIMS signal for quantitative measurements of boron content in the layer, boron implanted AlN sample was used as a reference. The boron content distribution along the growth direction is presented in Fig. 2(b). Under our growth conditions, 11% ($\pm$0.6%) boron incorporation has been obtained.

3.2. *Crystalline features of high boron containing layers*

In order to investigate structural quality of this heterostructure and also crystalline characteristics, the cross-section STEM was performed along [1 1 −2 0] zone axis. As shown in Fig. 3(a) the bright-field STEM image shows that the AlN/BAlN heterostructure has columnar polycrystalline features, such as the part in the rectangle box. By looking into the higher magnification image of the interface between 1st AlN and 1st BAlN in Fig. 3(c), it is clear that the 1st AlN layer is still monocrystalline. When BAlN growth starts the lattice is oriented along *c*-axis for around 5 nm, and then a tilt as large as 60° can be observed which means the structure tends to be polycrystalline and columnar growth starts. Better contrast of AlN and BAlN layers can be observed by *Z*-contrast HAADF-STEM images shown in Fig. 3(b), where layers with higher brightness represent AlN layers and darker layers present BAlN. The surface roughness height caused by this columnar feature is around 10–13 nm from STEM images.

The polycrystalline feature has been confirmed by HR-XRD results. In 2θ–ω scans shown in Fig. 4, a peak related to AlN (0 0 0 2) is located at 36.02°. Another peak at 37.98° should correspond to AlN (1 −1 0 1). Combining with STEM results, it can be explained that the first AlN layer was monocrystalline along c-axis. After the BAlN starts to grow, the structure becomes polycrystalline and epitaxial AlN layers grown afterwards also have lattice tilt so that X-ray diffraction signal from other facets arises. BAlN XRD peak was absent due to its polycrystalline feature especially with high boron incorporation.

This AlN/BAlN heterostructure has total thickness of 310 nm. The morphology is examined by AFM shown in Fig. 5. The surface was covered by columnar crystallites, confirming the STEM observations. The AFM scan area is 5 μm × 5 μm square. The structure has root-mean-square (RMS) of 3.3 nm. The average height of these columnar crystallites is around 10 nm which is in a good agreement with estimations from cross-section STEM images.

The polycrystalline feature was caused by the short diffusion length of boron atoms, which would challenge the applications of this material. From STEM image we observed that the monocrystalline critical thickness for BAlN with 11% boron is around 5 nm, above which the polycrystalline growth occurs. Meanwhile, the monocrystalline critical thickness is around 500 nm for BAlN of 2% boron as reported in the literature [10]. The larger the boron incorporated, the smaller the monocrystalline thickness of BAlN. Therefore, for different applications, a compromise can be achieved between thickness and boron composition. For example, for deep UV-DBRs, boron incorporation no more than 5% is enough to achieve high refractive index contrast [4,5]. Hence the boron content can be decreased to maintain BAlN layers (30–40 nm) monocrystalline. For ultra-thin layers such as MQWs or strain engineering superlattices, high boron incorporation can be used allowing a

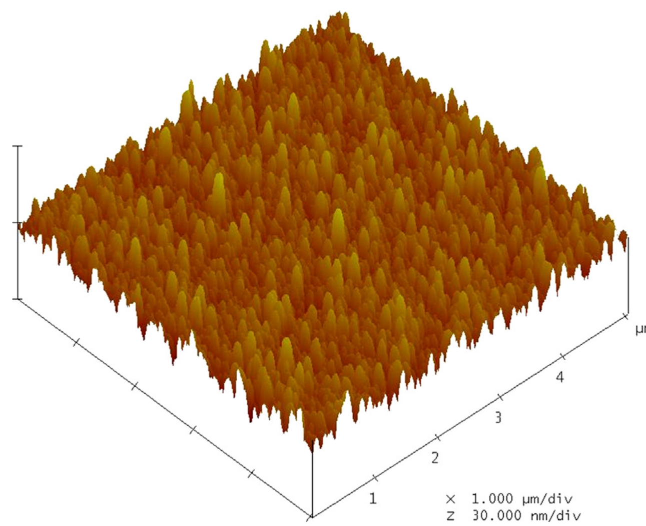

Fig. 5. Atomic force microscopy (AFM) image of 5-period AlN/BAlN heterostructure (310 nm for total thickness).

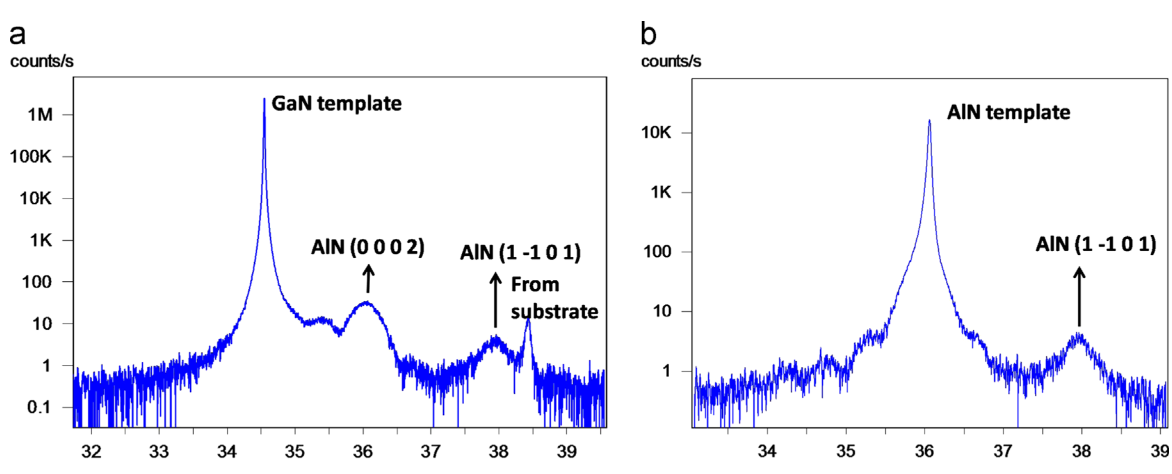

Fig. 4. h-XRD 2θ–ω scans of 5-period AlN/BAlN heterostructure grown on (a) GaN template and (b) AlN template.

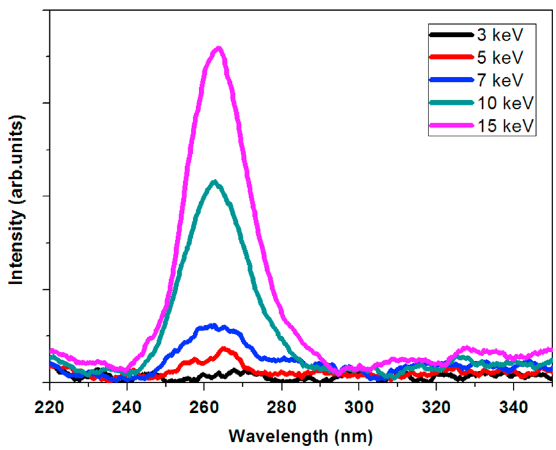

Fig. 6. Cathodoluminescence spectra at 77 K of 5-period AlN/BAlN heterostructure grown on AlN template.

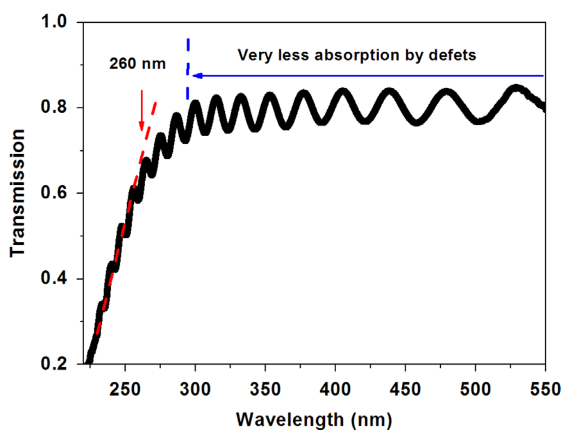

Fig. 7. Transmission spectrum at room temperature of 5-period AlN/BAlN heterostructure grown on AlN template.

large design freedom and it can still be kept as monocrystalline for its thin thickness (below 10 nm).

3.3. *Optical properties for deep UV wavelengths*

In order to study optical properties of this heterostructure containing high boron, cathodoluminescence (CL) and transmission spectra have been obtained for the sample grown on AlN template. As shown in Fig. 6, a well-defined emission peak at 262 nm emerges when the excitation power is above 7 keV. Meanwhile, as shown in Fig. 7, the optical absorption occurred at 260 nm which agrees well with CL results. For the wavelengths longer than 290 nm, the oscillation level of transmission fraction remains constant, which implies that there is very little absorption by defects in this region. The results obtained exhibit potentials to apply this material and structure for UV and deep UV devices.

It is noted that CL emission peak of AlN has not been detected due to limitation of our detector below 210 nm. In addition, since emission wavelength of BAlN is at 260 nm, the emission around 200 nm of AlN would be absorbed by the BAlN layers. As shown in Fig. 7 of transmission curve, there is a transmission drop at 260 nm, and below 260 nm, there is a large absorption.

Until now, few results have been reported on optical properties of BAlN material, especially for high boron containing layers. Theoretical calculations show that BAlN has strong bowing parameter (5.45 eV) [16], and for BGaN material the value of 9.2 eV has been experimentally obtained [17]. Based on this prediction, our BAlN layers should give an emission at around 225 nm. Here we observed a significant redshift of wavelength which might be due to high concentration of carbon impurities incorporated from TEB precursors (carbon density about 2×10^{19} cm^{-3} by SIMS). Since BAlN material is not as well studied as other III-nitrides, it still requires more experimental investigations for its optical properties.

4. Conclusion

5-period AlN/BAlN heterostructure with 11% boron has been grown by MOVPE. Good periodicity of two different layers has been achieved. The structure shows an emission peak and absorption edge at 260 nm which would be promising for UV-DBRs and deep UV devices. Although it still needs more efforts to improve crystalline quality and surface roughness caused by columnar growth of BAlN the studies in this work give better understanding of high boron containing layers and heterostructure growth, which would be helpful for the development of BAlGaN applications.

Acknowledgment

This work was supported by French ANR (Agence Nationale de la Recherche) in the framework of VESUVE project (ANR-11-BS03-0012).

References

[1] M.Haruyama, T. Shirai, H. Kurimoto, H. Kawanishi, in: Proceedings of the International Symposium on Blue Laser and Light Emitting Diode, Tokyo, 1996 p. 106.
[2] A.Y. Polyakov, M. Shin, W. Qian, M. Skowronski, D.W. Greve, R.G. Wilson, Growth of AlBN solid solutions by organometallic vapor-phase epitaxy, J. Appl. Phys. 81 (1997) 1715.
[3] A. Nakajima, Y. Furukawa, H. Yokoya, H. Yonezu, Growth of $B_xAl_{1-x}N$ layers using decaborane on SiC substrates, J. Cryst. Growth. 278 (2005) 437.
[4] S. Watanabe, T. Takano, K. Jinen, J. Yamamoto, H. Kawanishi, Refractive indices of $B_xAl_{1-x}N$ (x=0–0.012) and $B_yGa_{1-y}N$ (y=0–0.023) epitaxial layers in ultraviolet region, Physica Status Solidi C 0 (2003) 2691.
[5] M. Abid, T. Moudakir, G. Orsal, S. Gautier, A. En Naciri, Z. Djebbour, et al., Distributed Bragg reflectors based on diluted boron-based BAlN alloys for deep ultraviolet optoelectronic applications, Appl. Phys. Lett. 100 (2012) 051101.
[6] M. Abid, T. Moudakir, Z. Djebbour, G. Orsal, S. Gautier, A. En Naciri, et al., Blue–violet boron-based Distributed Bragg Reflectors for VCSEL application, J. Cryst. Growth. 315 (2011) 283.
[7] J.H. Edgar, D.T. Smith, C.R. Eddy, C.A. Carosella, B.D. Sartwell, c-Boron–aluminum nitride alloys prepared by ion-beam assisted deposition, Thin Solid Films. 298 (1997) 33.
[8] L. Liljeholm, J. Olsson, Electrical characterization of wurtzite (Al,B)N thin films, Vacuum 86 (2011) 466.
[9] T. Akasaka, Y. Kobayashi, T. Makimoto, Nonpolar AlBN (1120) and (1100) films grown on SiC substrates, Appl. Phys. Lett. 91 (2007) 041914.
[10] T. Akasaka, T. Makimoto, Flow-rate modulation epitaxy of wurtzite AlBN, Appl. Phys. Lett. 88 (2006) 041902.
[11] H. Kawanishi, T. Honda, Fabrications of BAlGaInN multi-layer or quantum well structure for blue to UV light emitter and its applications to optical devices, Photonics Based on Wavelength Integration and Manipulation 2 (2005) 19.
[12] A.Y. Polyakov, M. Shin, M. Skowronski, D.W. Greve, R.G. Wilson, A.V. Govorkov, et al., Growth of GaBN ternary solutions by organometallic vapor phase epitaxy, J. Electron. Mater. 26 (1997) 237.
[13] X. Li, S. Sundaram, Y. El Gmili, T. Moudakir, F. Genty, S. Bouchoule, et al., BAlN thin layers for deep UV applications, in: Proceedings of the E-MRS Spring Meeting, 2014.
[14] S. Gautier, C. Sartel, S. Ould-Saad, J. Martin, A. Sirenko, A. Ougazzaden, GaN materials growth by MOVPE in a new-design reactor using DMHy and NH_3, J. Cryst. Growth. 298 (2007) 428.
[15] J. Kim, Z. Lochner, M.-H. Ji, S. Choi, H.J. Kim, J.S. Kim, et al., Origins of unintentional incorporation of gallium in InAlN layers during epitaxial growth, part II: effects of underlying layers and growth chamber conditions, J. Cryst. Growth. 388 (2014) 143.
[16] S. Azzi, A. Zaoui, M. Ferhat, On the importance of the band gap bowing in Boron-based III–V ternary alloys, Solid State Commun. 144 (2007) 245.
[17] A. Ougazzaden, S. Gautier, T. Moudakir, Z. Djebbour, Z. Lochner, S. Choi, et al., Bandgap bowing in BGaN thin films, Appl. Phys. Lett. 93 (2008) 083118.